

2016

Robust fuzzy-sliding mode based UPFC controller for transient stability analysis in autonomous wind-diesel-PV hybrid system

Asit Mohanty

Sandipan Patra

Prakash K. Ray

Follow this and additional works at: <https://arrow.tudublin.ie/engscheleart2>



Part of the [Electrical and Computer Engineering Commons](#)

This Article is brought to you for free and open access by the School of Electrical and Electronic Engineering at ARROW@TU Dublin. It has been accepted for inclusion in Articles by an authorized administrator of ARROW@TU Dublin. For more information, please contact arrow.admin@tudublin.ie, aisling.coyne@tudublin.ie, gerard.connolly@tudublin.ie.



This work is licensed under a [Creative Commons Attribution-NonCommercial-Share Alike 4.0 License](#)

Robust fuzzy-sliding mode based UPFC controller for transient stability analysis in autonomous wind-diesel-PV hybrid system

Asit Mohanty¹, Sandipan Patra² ✉, Prakash K. Ray³

¹Department of Electrical Engineering, CET Bhubaneswar, Bhubaneswar, India

²School of Electrical and Electronic Engineering, Dublin Institute of Technology, Ireland

³Department of Electrical and Electronics Engineering, IIIT Bhubaneswar, Bhubaneswar, India

✉ E-mail: patra.sandipan@gmail.com

ISSN 1751-8687

Received on 9th September 2014

Revised on 16th October 2015

Accepted on 30th October 2015

doi: 10.1049/iet-gtd.2015.1000

www.ietdl.org

Abstract: This study presents a comparative study of transient stability and reactive power compensation issues in an autonomous wind–diesel–photovoltaic based hybrid system (HS) using robust fuzzy-sliding mode based unified power flow controller (UPFC). A linearised small-signal model of the different elements of the HS is considered for the transient stability analysis in the HS under varying loading conditions. An IEEE type 1 excitation system is considered for the synchronous generator in the HS, with negligible saturation characteristic, for detailed voltage stability analysis. It is noted from the simulation results that the performance of UPFC is superior to static VAR compensator and static synchronous compensator in improving the voltage profile of the HS. Further, fuzzy and fuzzy-sliding mode based UPFC controller is designed in order to improve the transient performance. Simulation results reflect the robustness of the proposed fuzzy-sliding mode controller for better reactive power management to improve the voltage stability in comparison with the conventional PI and fuzzy-PI controllers. In addition to this, system stability analysis is performed based on eigenvalue, bode and popov for supporting the robustness of the proposed controller.

1 Introduction

The advancement in distributed generation (DG) technology such as fuel cell (FC), wind turbine, photovoltaic (PV), and new innovation in power electronics, increasing electricity requirement, utility restructuring, environmental policy, increase in fuel price and the depletion of fossil fuels and customer demands for better power quality (PQ) and reliability are forcing the power industry to utilise them as an alternative energy option to central power system. Hence, DG can fulfil customer's demand in stand-alone as well as grid-connected mode as per situation requirements and the surplus power generation can be fed to the grid thereby increasing the reliability of power supply. However, the undesirable environmental characteristic variations in wind speed and solar radiations make wind and PV power generation unreliable and create PQ problems. Hence, these sources may be connected to the conventional power generating resources for increasing quality and reliability of power supply [1, 2].

Wind–diesel–PV systems are widely used as hybrid system (HS) in which a wind turbine combines with a diesel generator and PV system to provide power in remote places. Normally a synchronous generator (SG) is preferred to act as diesel generator and induction generator is used in wind turbine for improved performance [3–6]. Induction generators are advantageous in comparison with SG due to their rugged characteristics and they need reactive power for their operation. A system having SG, induction generator and PV connected to load, become complex where the induction generator and loads need the reactive power and it is provided by the SG and PV system. However, the reactive power supplied by the SG and PV inverter fail to meet the requirement and therefore a big gap is created between the demand and generation of reactive power. This may lead to voltage instability in the power system.

The use of capacitor banks to improve voltage stability and to compensate the reactive power in the system is presented in [7–9]. However, fixed capacitors fail to deliver the reactive power requirement and hence flexible AC transmission system (FACTS) devices such as static VAR compensator (SVC), static synchronous compensator (STATCOM), unified power flow controller (UPFC)

are commonly used for reactive power compensation [10–17]. These devices are also used for voltage and angle stability studies of power system [18–23].

The greatest advantage of dynamic stability design approach of feedback linearisation is that it transforms non-linear system dynamics into linear one which is a reduced-order linear system. For the reduced-order system a linear controller can be designed so that the autonomous HS should be stable and have zero dynamics. There are several controllers designed by using adaptive control methods [24–27]. Moreover robust control methods were utilised to design the controllers such as variable structure control [28, 29] and Gain scheduling [25]. Sliding mode control (SMC) is a novel controller which uses variable structure control method and is widely used in robotics applications and control of semi-active suspension systems [30]. The typical characteristics of the SMC is that it is discontinuous and forces the system variable to slide along a pre-defined sliding surface to maintain stability. The controller is robust and can handle modelling inaccuracies. Though fuzzy-PI control is another adaptive control method which has been cited by many researchers [31]. Fuzzy SMC is considered in this paper for its better performance in terms of accuracy, overshoot and settling time. The fuzzy-SMC controller is designed using a fuzzy inference system.

This work mainly focuses on a UPFC based controller with fuzzy-SMC for reactive power control and for a better damping control in a wind–diesel–PV HS. A comparison of FACTS devices for reactive power control also presented in this paper. Transient stability analysis for each measuring parameter with incorporation of FACTS devices are compared. This manuscript also presented the system stability analysis using different techniques.

2 System configuration and mathematical modelling of hybrid power system

In the proposed HS which clearly depicted in Fig. 1, the active power is supplied by the induction and SG where the reactive power need of the induction generator and the load is met by the FACTS devices such as SVC, STATCOM and UPFC. The HS parameters are

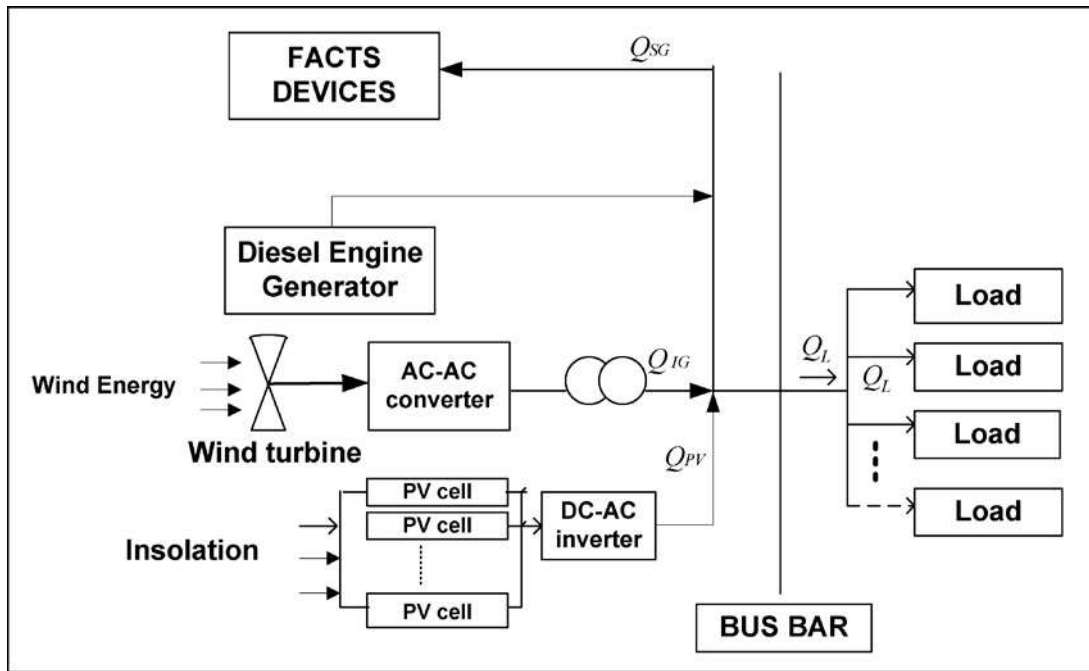


Fig. 1 Flow of Reactive power in wind–diesel-PV HS

mentioned in appendix Table 3. Variable speed wind generation system, photovoltaic system whose output power fluctuates according to the weather conditions are considered for different case studies. PV is added to the system to increase the reliability and robustness of the system. The amount of reactive power supplied or absorbed by the PV system depends upon the targeted power factor which can be controlled within a range of 0.85 lagging to 0.85 leading.

For wind energy conversion system SG with IEEE type 1 excitation system is considered and it is acting as a local grid for IG. The mathematical modelling and different subsystems such as wind–diesel-PV, FACTS controllers (SVC, STATCOM and UPQC) are described in the following sections.

The reactive power balance equations of the HS under steady-state conditions are mentioned below.

$$Q_{PV} + Q_{SG} + Q_{COM} = Q_L + Q_{IG} \quad (1)$$

Q_{PV} , reactive power generated by PV; Q_{SG} , reactive power generated by SG; Q_{COM} , reactive power generated by the FACTS device; Q_L , reactive power needed by the load; Q_{IG} = reactive power needed by the induction generator.

When the system experiences a change of load ΔQ_L the other parameters also experience change in reactive power.

$$\Delta Q_{PV} + \Delta Q_{SG} + \Delta Q_{COM} = \Delta Q_L + \Delta Q_{IG} \quad (2)$$

$\Delta Q_{PV} + \Delta Q_{SG} + \Delta Q_{COM} - \Delta Q_L - \Delta Q_{IG}$, surplus Reactive Power of the System.

The surplus reactive power affects the system voltage in two ways, it increases the electro magnetic energy absorption of induction generator and increases the reactive load consumption.

In differential and Laplace form the equation can be written as [5]

$$\Delta Q_{PV} + \Delta Q_{SG} + \Delta Q_{COM} - \Delta Q_L + \Delta Q_{IG} = \frac{d}{dt}(\Delta E_m) + D_V \Delta V \quad (3)$$

$$\Delta V(S) = \frac{K_V}{1 + ST_V} [\Delta Q_{SG}(S) + \Delta Q_{COM}(S) + \Delta Q_{PV}(S) - \Delta Q_L(S) - \Delta Q_{IG}(S)] \quad (4)$$

where $T_V = (2H_r/D_V)V^0$ and $K_V = (1/D_V)$.

The dynamic behaviours of practical WTG, DEG, PV etc. can be simulated by employing higher-order mathematical models with non-linearity which may include associated power conditioners and controllers. Therefore, for larger disturbances, the detail modelling of the system components should be considered for the transient analysis. However, in the current study, a small-signal analysis for small change in load/wind speed/solar radiation is considered as input disturbances into the HS. Hence, rather than taking the non-linear/detail modelling, a linearised system components is presented for the analysis. Actually, in the expansion of mathematical model by Taylor's series, the higher order terms are neglected to obtain a linearised model of the components of the HS. Of course, in this method of linearisation, some dynamics/properties may be lost. However, since the severity of disturbance is small in nature, and a small-signal analysis is proposed, the main objective for study of system response and stability will not be much affected. Hence, the power losses and controllers are not considered in different cases of the proposed study and the linearised system modelling is developed based on the small-signal stability analysis [3, 5, 6].

2.1 Mathematical model of SG

The SG is mainly used as primary source of electric supply and an alternative of grid power. SG supply reactive power to the system which can control the reactive power requirement of the HS. SG when connected to wind turbine must be controlled carefully to prevent the rotor speed accelerating through synchronous speed.

Commonly used SG equation is given by

$$Q_{SG} = \frac{(E'_q V \cos \delta - V^2)}{X'd} \text{ (Transient)} \quad (5)$$

For small change the same equation is written as

$$\Delta Q_{SG} = \frac{V \cos \delta}{X'd \Delta E'_q} + \frac{E'_q \cos \delta - 2V}{X'd \Delta V} \quad (6)$$

In Laplace form the equation can be written as

$$\Delta Q_{SG}(S) = K_a \Delta E'_q(S) + K_b \Delta V(S) \quad (7)$$

where K_a and K_b are $K_a = (V \cos \delta / X'd)$ and $K_b = (E'_q \cos \delta - 2V / X'd)$.

2.2 IEEE type 1 excitation system

To drive the synchronous machine direct current should be provided to its field winding which is produced from excitation system. The field voltage and the field current are also controlled by the excitation system which is represented by a single time constant automatic high gain AVR System. Though there are different types of excitation systems, IEEE type-1 excitation system as shown in Fig. 2a is found to be suitable for this isolated HS.

The mathematical modelling of the excitation system is based on

$$\dot{E}_{fd} = (-E_{fd} + K_A(V_{ref} - V))/T_A \quad (8)$$

2.3 Flux linkage of SG

For a round rotor synchronous motor the flux linkage equation

$$\frac{d}{dt}(\Delta E'_q) = \frac{(\Delta E'_{fd} - \Delta E'_q)}{T'_{do}} \quad (9)$$

$$E'_q = \left(\frac{X_d}{X'_d}\right)E'_q - \left(\frac{X_d - X'_d}{X'_d} \frac{dV}{dt} \cos \delta\right) \quad (10)$$

For small incremental change Laplace transform is written as

$$(1 + sT_G)\Delta E'_q(s) = K_e\Delta E'_{fd}(s) + K_f\Delta V(s) \quad (11)$$

where $T_G = (X'_d T'_{do}/X_d)$, $K_e = (X'_d/X_d)$ and $K_f = ((X_d - X'_d)\cos \delta/X_d)$.

2.4 Mathematical modelling of induction generator

In proposed isolated system the reactive power is mainly provided by the SG. Reactive power requirement of IG is changing with the wind speed variation. To study the effect of this variable slip model of IG is used.

The state space equation for svc controller in a standard form can be written as [3]

$$\dot{x} = [A]\bar{x} + [B]\bar{u} + [C]\bar{p} \quad (12)$$

$$\bar{x} = [\Delta E'_{fd} \Delta V_a \Delta V_f \Delta E'_q \Delta B_{SVC} \Delta B'_{SVC} \Delta \alpha \Delta V]^T$$

$$\bar{u} = [\Delta V_{ref}] \quad (13)$$

$$\bar{p} = [\Delta Q_L \quad \Delta PIW]^T$$

Matrix [A], [B], [C] can be calculated and are of same order as \bar{x} , \bar{u} and \bar{p} .

2.5 Modelling of PV system

The PV cell is basically a p-n junction device that converts the amount of incidence solar radiation into electrical power. In the proposed system small signal equivalent model of PV is consider, where it is providing reactive power into the system. Fig. 2b reflects the block diagram representation of reactive power generation from the PV system.

If Φ is the power angle between the grid voltage and the inverter output current and δ is the load angle between the grid voltage (V) and the inverter output voltage (E)

$$E = V + jX_S I \quad (14)$$

$$E \sin(\delta) = X_S I \cos(\phi) \quad (15)$$

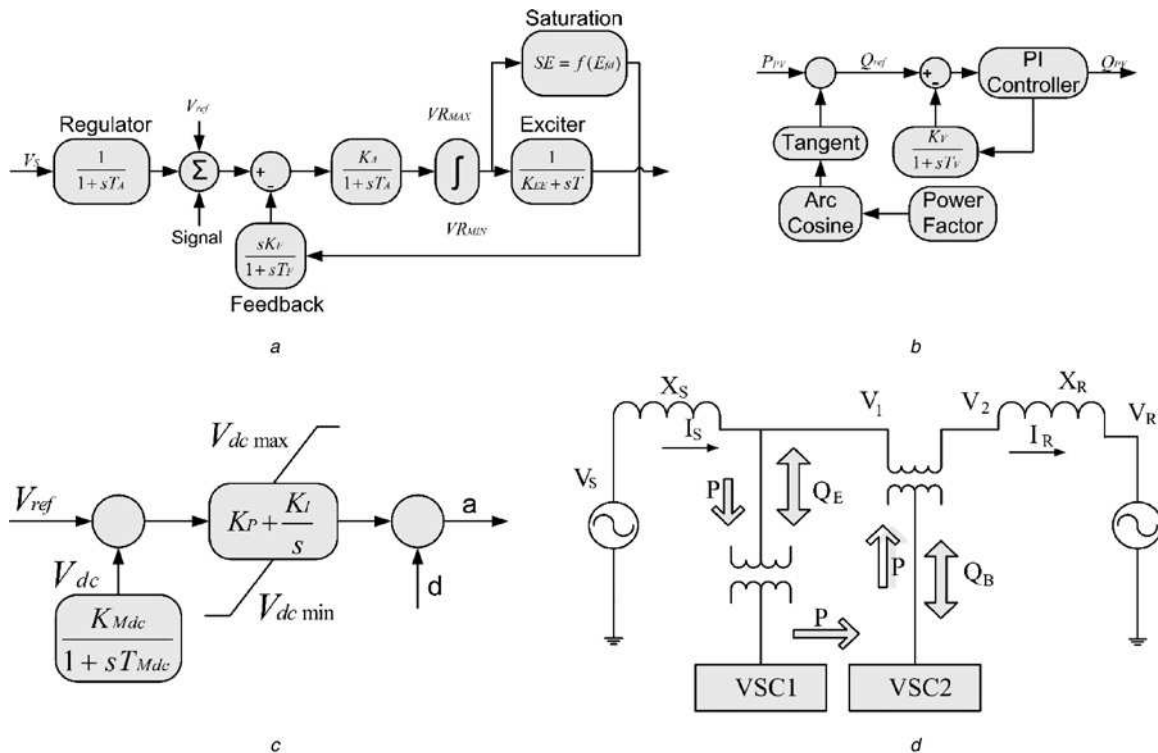


Fig. 2 Mathematical modelling of the HS

- a IEEE type-1 excitation system
- b Reactive power output (Qpv)
- c STATCOM with PWM voltage control
- d Block diagram of UPFC controller

Active power (P) provided by the converter to the grid can be expressed as

$$P = VI \cos(\phi) = \frac{VE}{X_S} \sin(\delta) \quad (16)$$

The reactive power provided by the PV Converter to the grid

$$Q = \frac{VE}{X_S} \cos(\delta) - \frac{V^2}{X_S} = \frac{V}{X_S} (V \cos(\delta) - V) \quad (17)$$

2.6 Static VAR compensator

In case SVC supplies the reactive power which is $Q_{SVC} = V^2 B_{SVC}$. Laplace transform of the said equation for a small perturbation [16]

$$\Delta Q_{SVC}(S) = K_C \Delta V(S) + K_d \Delta B_{SVC}(S) \quad (18)$$

where $K_C = 2VB_{SVC}$ and $K_d = V^2$.

$$\Delta B_{SVC}(S) = \frac{1}{1 + sT_d} \Delta B_{SVC}(S) \quad (19)$$

$$\Delta B_{SVC}(S) = \frac{K_\alpha}{1 + sT_\alpha} \quad (20)$$

$$\Delta \alpha = \frac{K_R}{1 + sT_R} [\Delta V_{ref}(s) - \Delta V(S)] \quad (21)$$

2.7 Static synchronous compensator

STATCOM small signal model is showing in Fig. 2c. For this STATCOM compensator gain regulator K_R is used for control mechanism [14]. In case of SVC the small change in reactive power [15] is based on ΔV and ΔB_{SVC} and in STATCOM the reactive power change depends on ΔV and $\Delta \alpha$.

The steady state equation of reactive power provided by STATCOM is given by

$$Q + V^2 B - KV_{dc} VB \cos(\delta - \alpha) + KV_{dc} VG \sin(\delta - \alpha) = 0 \quad (22)$$

Taking incremental change it can be found out

$$\Delta Q_{STATCOM} = KV_{dc} VB \sin \alpha - KV_{dc} B \cos \alpha \quad (23)$$

The angle δ value is neglected

$$\begin{aligned} \Delta Q_{STATCOM}(S) &= K_J \Delta \alpha(S) + K_K \Delta V(S) \\ K_k &= KV_{dc} VB \sin \alpha \\ K_L &= KV_{dc} VB \cos \alpha \end{aligned} \quad (24)$$

2.8 Unified power flow controller

UPFC is a commonly used FACTS controller for reactive power compensation. In this proposed HS UPFC is used for reactive power compensation with robust control strategies. The small signal mathematical model is considered. Fig. 2d shows the modelling of UPFC controller and power flow through it.

It has been assumed that the series and shunt impedances of UPFC are pure reactances. P_{sh} and Q_{sh} are with the shunt voltage sources while P_i , Q_i , P_j and Q_j represent the series voltage sources. The injected powers depend on the injected voltages and bus voltages also. Buses i and j are taken as load buses in the load flow analysis. They are taken with some modifications as the injected powers are not constant. The reactive power injected by UPFC

controller can be derived [32] as

$$\frac{dQ_j}{dt} = \frac{dQ_j}{d\delta} \frac{d\delta}{dt} + \frac{dQ_j}{dV_{m2p}} \frac{dV_{m2p}}{dt} \quad (25)$$

From these equations it can be said that the reactive power injected by UPFC depends upon V_{m2p} and angle δ which are proportional to the voltage at the point of connection of UPFC

$$\Delta Q_{UPFC} = K_J \Delta \delta(S) + K_k \Delta V(S) \quad (26)$$

2.9 Robust controller design for reactive power control

The controller is the vital component in the load frequency control loop. The controller is designed such that the error can be minimised in the least time possible. Fuzzy logic control has been used in several control scenarios successfully. It is widely used in non-linear systems as well. However, it lacks in stability and performance in presence of modelling uncertainties and disturbances. In such scenarios robust control methods such as SMC are useful, which can handle modelling uncertainties and disturbances. Hence, in this paper the fuzzy logic controller is designed using SMC paradigm to achieve a fast and stable controller.

2.9.1 Sliding mode control: SMC is a robust control approach appropriate for control of time-variant systems in the presence of external disturbances [14]. SMC uses a high-speed switched feedback control to sustain the control variable on the sliding surface. The gain in the feedback path switches between two values according to a rule that depends on the value of the variable at each instant. The aim is to drive the plant's state trajectory onto a pre-specified surface in the state space and to maintain it on this surface for subsequent time. A Lyapunov approach is used to characterise the switched control design that will maintain the plant state on the surface after interception. Lyapunov method is usually used to determine the stability properties of an equilibrium point without having to solve the state equation. Stability is assured in the Lyapunov method by ensuring that the function is positive definite if it is negative and it is negative definite if it is positive.

The design procedure involves two steps:

Selection of a sliding surface and computation of a control law to force the system's trajectory towards and keeping it on the sliding surface.

Considering a system defined by the state-space equation

$$\ddot{x}(t) = f(x, t) + u(t) \quad (27)$$

where x is the state vector, u is the control vector which controls the state vector. In this case the state vector is the system frequency. The estimation error on $f(x, t)$ is bounded by the function

$$|\hat{f}(x, t) - f(x, t)| \leq F(x, t) \quad (28)$$

$\hat{f}(x, t)$ is the estimated value for $f(x, t)$. The sliding variable is defined by

$$s(x, t) = \left(\frac{d}{dt} + \delta \right) \tilde{x}(t) \quad (29)$$

Here δ is a positive constant that defines the bandwidth of the system and $\tilde{x}(t) = x(t) - x_d(t)$. Here $x_d(t)$ is the desired state. Hence, here the sliding variable can be defined as

$$s(t) = \left(\frac{d}{dt} + \gamma \right) \tilde{x}(t) = \dot{\tilde{x}}(t) + \gamma \tilde{x}(t) \quad (30)$$

Differentiation of the sliding variable gives

$$\dot{s}(t) = \ddot{\tilde{x}}(t) - \dot{x}_d(t) + \gamma \dot{\tilde{x}}(t) \quad (31)$$

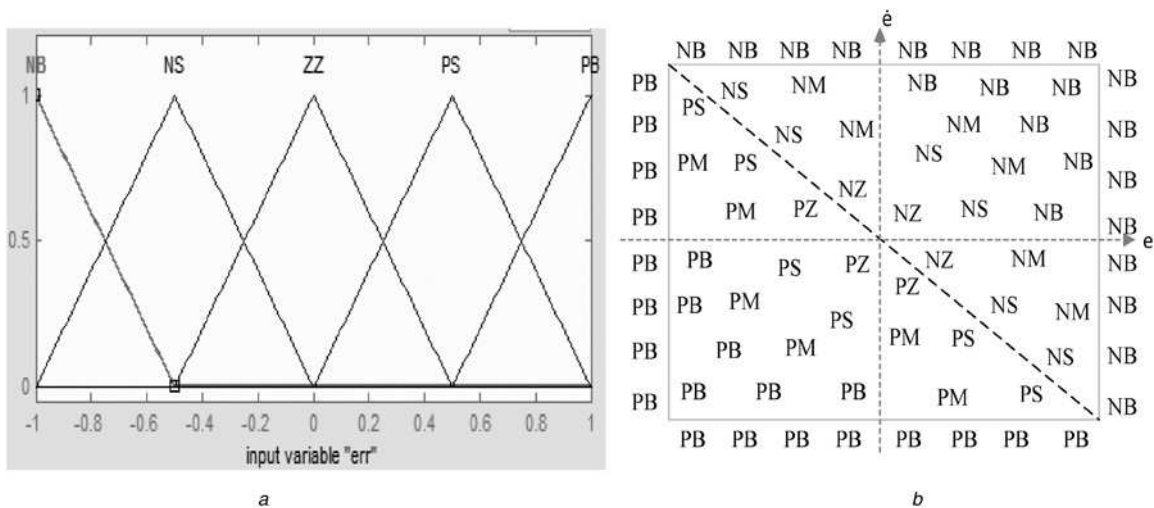


Fig. 3 Fuzzy logic control
a Input membership function
b Rules of fuzzy sliding mode controller

This implies

$$\dot{s}(t) = f(x, t) + u(t) - \ddot{x}_d(t) + \gamma \dot{\tilde{x}}(t) \quad (32)$$

The control law is then formulated by the use of Lyapunov stability theorem. The condition in (10) states that the squared distance to the surface as measured by s^2 decreases along all system trajectories.

$$\frac{1}{2} \frac{d}{dt} s^2 \leq -\eta |s| \quad (33)$$

where η is a strictly positive constant. The condition constrains trajectories towards the surface $s(x, t)$. Hence, the control law can now be defined as

$$u(t) = \hat{u}(t) - k(x, t) \text{sgn}(s(t)) \quad (34)$$

By choosing the upper bounds, $k(x, t)$ large enough such as

$$k(x, t) = F(x, t) + \eta \quad (35)$$

Ensures the satisfaction of condition

$$\begin{aligned} \frac{1}{2} \frac{d}{dt} (s(t)^2) &= \dot{s}(t)s(t) \\ &= (f(x, t) - \hat{f}(x, t))s(t) - k(x, t)|s(t)| \leq -\eta |s(t)| \end{aligned} \quad (36)$$

Here $F(x, t)$ is a known bound for error estimation. Thus within a finite time the system trajectory is driven to the sliding surface and error reduces to zero.

2.9.2 Fuzzy sliding mode controller design: Fuzzy logic control is one of the several alternatives for feedback adaptive controllers. It is based on the ‘expert experience’ of human operators and is designed using ‘linguistic variables’ that are used and understood by humans. Here it is modelled by a set of if-then rules which are derived from the SMC paradigm [15]. The two inputs are error in system frequency (f) and change in error (\dot{f}).

The crisp values are normalised so that they match the scale of the fuzzifier. The five linguistic variables for two inputs of f and \dot{f} are NB, NS, ZZ, PS and PB (negative big, negative small, zero, positive small and positive big). The membership functions for both inputs and output are used to convert the normalised values into mapped elements (linguistic variables) and vice versa. The membership function is shown in Fig. 3a. To model the FLC on the basis of sliding mode algorithm, the rule base is designed such

that the control output is positive below the sliding surface and negative above it. Let $K_{\text{fuzz}}(f, \dot{f})$ be the control of the FLC. The working principle of the FLC can then be given by

$$u = -K_{\text{fuzz}}(f, \dot{f}) \cdot \text{sgn}(s) \quad (37)$$

The resulting rules are illustrated in Fig. 3b where outputs close to the sliding surface are smaller and increase in magnitude further away from it. The linguistic variables used in the rule base are P, N, S, M, B, Z (positive, negative, small, medium, big, zero). The control output is then obtained by using a defuzzification method. The denormalisation method is used to obtain the final control output to be used on the LFC system. Normalisation and denormalisation are linear transformations that convert the crisp values into normalised values on the phase plane and vice versa. On the system phase plane we have $\lambda \cdot e + \dot{e} = 0$. In the normalised phase plane we have $\lambda_N \cdot e_N + \dot{e}_N = 0$. This implies

$$e_N = e \cdot N_e; \quad \dot{e}_N = \dot{e} \cdot N_{\dot{e}}; \quad (38)$$

where $N_e, N_{\dot{e}}$ are normalisation factors. Hence we can obtain

$$\lambda = \lambda_N \cdot \frac{N_e}{N_{\dot{e}}} \quad (39)$$

Nayak *et al.* used fuzzy PI as the load frequency controller in a three-area hybrid power system [10]. The fuzzy PI is used in the three-area system being considered here and the performance of the FLC and the fuzzy sliding mode controller are compared.

3 Simulation study and analysis

In this section the transient response of isolated wind–diesel-PV system are presented. The system is simulated for constant wind speed and as well as for variable wind speed and variable solar insolation. Three different configuration of the said system are made with three reactive power controllers SVC, STATCOM and UPFC. To make the system more reliable and robust a PV model has been added which has capability to supply real and reactive power to the system. Transient responses of the three controllers are compared in terms of first swing amplitude and settling time. Values of constants are derived from the data mentioned in the Appendix in Tables 3 and 4.

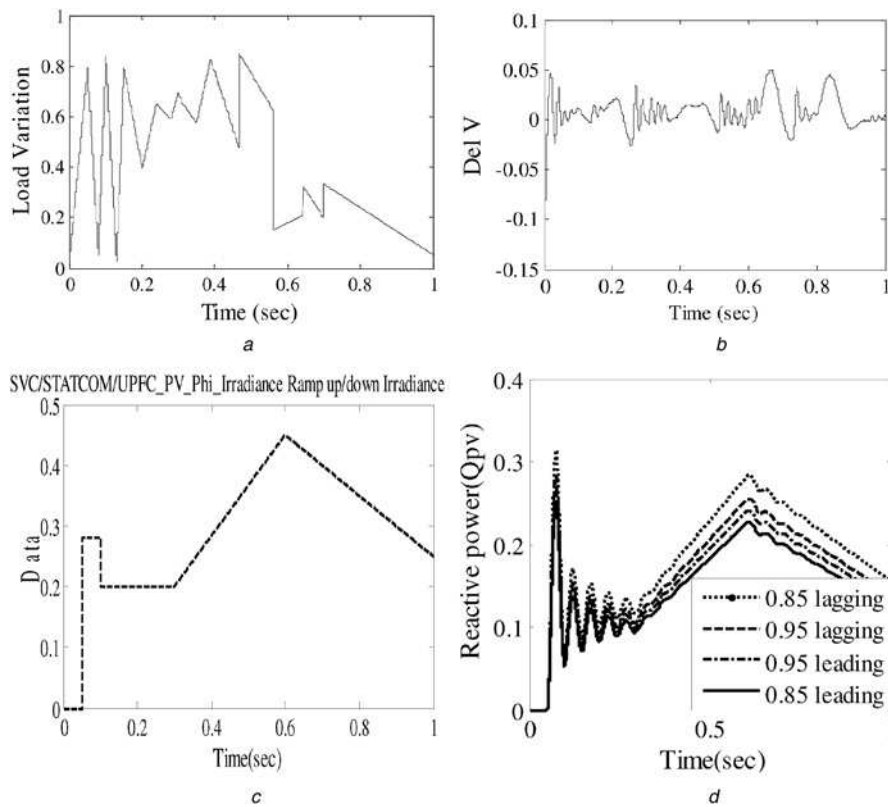


Fig. 4 Variation of input parameters and their effect
a, b Random variation in load and its system response without any controller
c, d Input solar insolation signal and reactive power produced by the PV generation

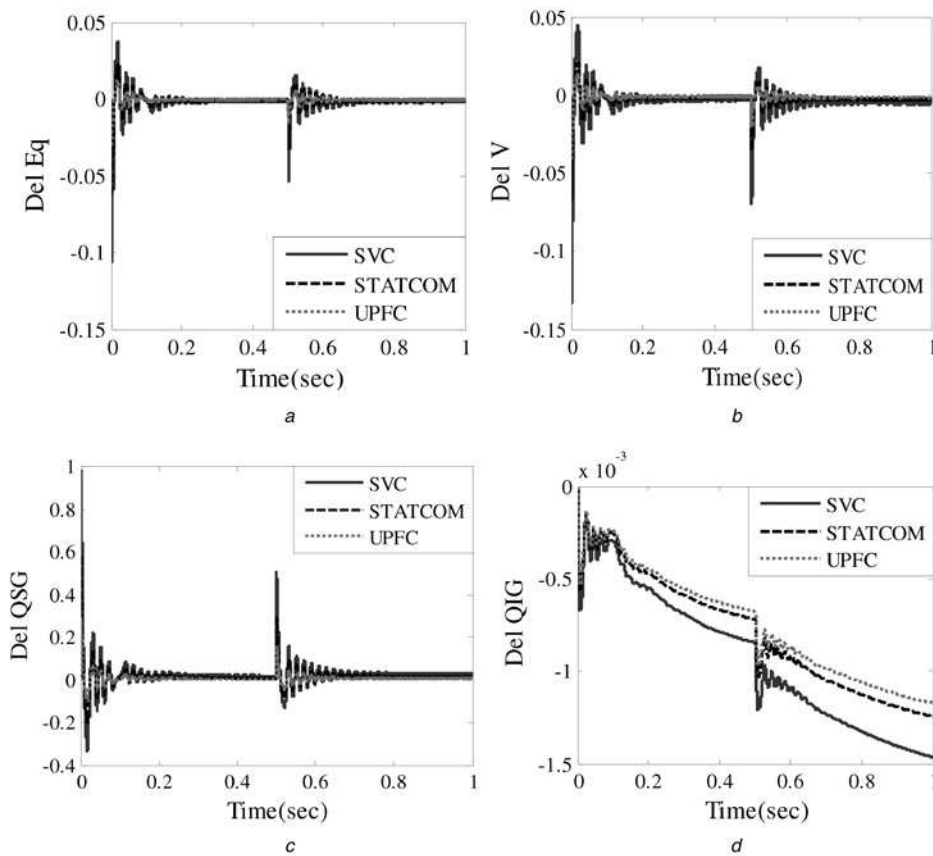


Fig. 5 Transient Responses of wind-diesel-PV system with 2% step increase of load with variable slip and variable insolation
 Variation of the system parameters *a* armature voltage *b* terminal voltage *c* reactive power of SG and *d* reactive power of induction generator

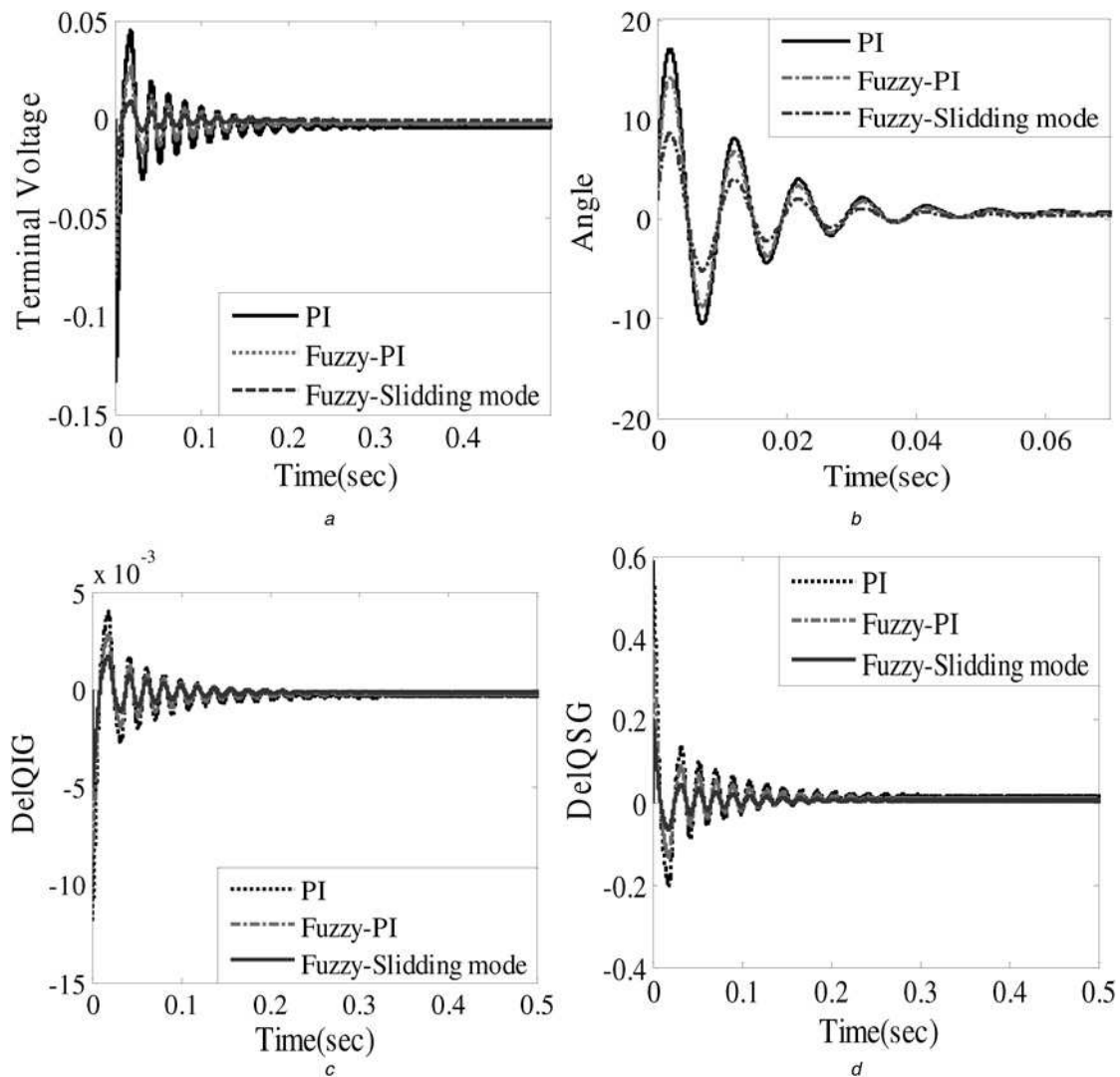


Fig. 6 Comparison of transient responses of wind-diesel-PV system based on UPFC controller with 2% step increase of load with PI, fuzzy-PI and fuzzy-sliding mode technique

Variation of the system parameters *a* terminal voltage *b* firing angle *c* reactive power of induction generator and *d* reactive power of SG

3.1 Transient stability analysis

The complete simulation was carried away taking the FACTS Controllers in the wind-diesel-PV hybrid power system in MATLAB/Simulink environment. Detailed analysis of system parameters with respect to reactive power and voltage control of the isolated HS was considered with a step load change of 2% and random variation of load. The random variation of the load profile is shown in Fig. 4*a*. The oscillation in the change in voltage profile of the hybrid power system without any controller is shown in Fig. 4*b*. The analysis is also performed under varying solar insolation as shown in Fig. 4*c*. The reactive power supply from PV system to the hybrid system is shown in Fig. 4*d*. The variation of all the system parameters such as reactive power of SG (ΔQ_{SG}), induction generator (ΔQ_{IG}), change in reactive power of PV (ΔQ_{PV}), variation in terminal voltage (ΔV), Variation in armature voltage (ΔE_q) etc. as shown in Figs. 5*a-d*. The responses shown in Figs. 5*a-d* clearly show the settling time and first swing amplitudes of the three controllers at constant slip and load increase of 2% with a variation in solar insolation. Simulation results for the wind-diesel-PV system was carried out to analyse the impact of PV in maintaining the reliability and robustness of the system. The maximum deviations of different parameters with 2% step increase of load is compared in Table 1 in Appendix. It is observed that increase in reactive power load in wind-diesel-PV

system is met by the SVC, STATCOM and UPFC controllers. It is also analysed that with incorporation of PV in the HS has enhanced the stability and reliability. It is observed from the transient responses that the peak overshoot, settling time is less in case of UPFC as compared with that of SVC and STATCOM.

Further in order to enhance the performance of the UPFC controller, Fuzzy based PI controller and fuzzy based SMC is designed to improve the reactive power compensation and transient voltage stability of the HS. It is found that the oscillations are damped out in around 0.15, 0.18 and 0.2 s for UPFC with fuzzy-sliding mode, fuzzy-PI and conventional PI controllers, respectively. From Figs. 6*a-d* it can be observed that the system performance is best in case of UPFC with Fuzzy-sliding mode in comparison with other two controllers. The Wind- Diesel-PV system is subjected to variable insolation and the simulations show the same trend and proves the superiority of UPFC because of comparatively better reactive power compensation by the PV system.

To prove the robustness of the controllers, the analysis is further tested for random variation in load as shown in Fig. 4*a*. The variation of all the system parameters such as reactive power of SG (ΔQ_{SG}), Variation in armature voltage (ΔE_q), Variation in reactive power of UPFC (ΔQ_{UPFC}), and Variation in terminal voltage (ΔV) etc. are shown in Figs. 7*a-d*, respectively, in presence of the controllers under random variation in load. It is

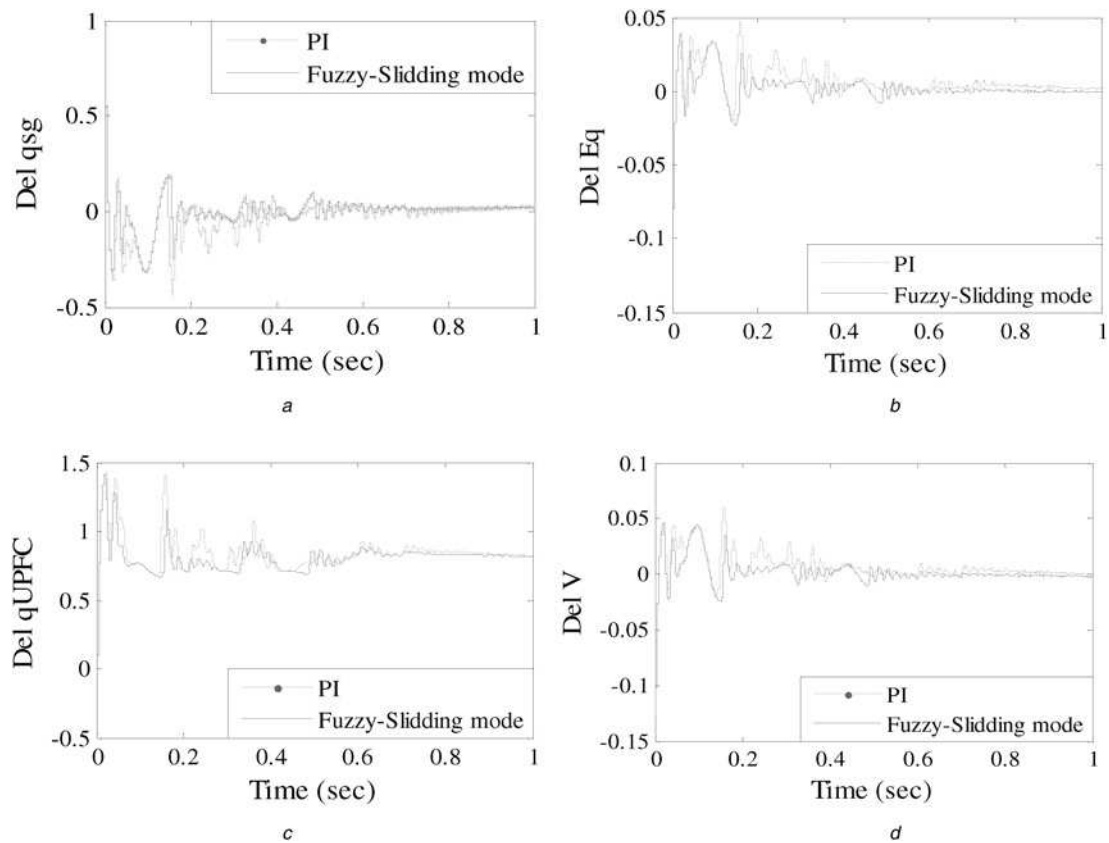


Fig. 7 Transient responses of wind–diesel-PV system based on UPFC controller with random variation of load with PI and fuzzy-sliding mode technique
Variation of the system parameters *a* reactive power of SG *b* armature voltage *c* reactive power of UPFC *d* terminal voltage

observed from the transient response of the wind–diesel-PV system for the different parameters that the oscillations are minimised because of the proposed controllers and are subsequently die out with minimum settling time and overshoots. This analysis also reflects that Fuzzy-SMC is performing better than the other controllers even under larger variation in load profile of the system. It is also observed the reactive power compensation is effectively done by SVC, STATCOM and UPFC controllers in order to have an improved system transient performance and better stability. Of course, the peak overshoot, settling time is less in case of UPFC as compared with that of SVC and STATCOM as being observed in the previous case studies.

3.1.1 Quantitative analysis: In this section a quantitative analysis is carried out for different FACTS controllers which are shown in above section. A comparison of peak overshoot is provided in Fig. 8 for different FACTS controllers. It is observed that UPFC provides minimum peak overshoot and settling time is less than other two controllers. Further, similar comparative analysis is performed in the presence of conventional PI, fuzzy-PI and fuzzy-SMC with UPFC. Fuzzy SMC is observed to show better performance in peak overshoot and settling time as compared with the other controllers. The tuned values of PI controllers for SVC, STATCOM and UPFC are represented in Table 1. During observation it was found that the size of the

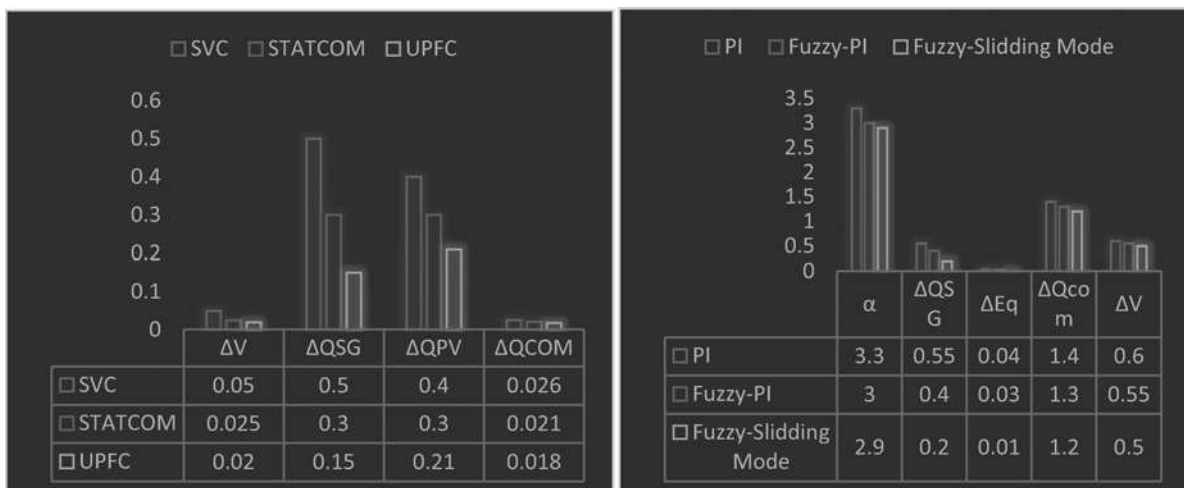


Fig. 8 Comparison of maximum peak overshoots of different controllers

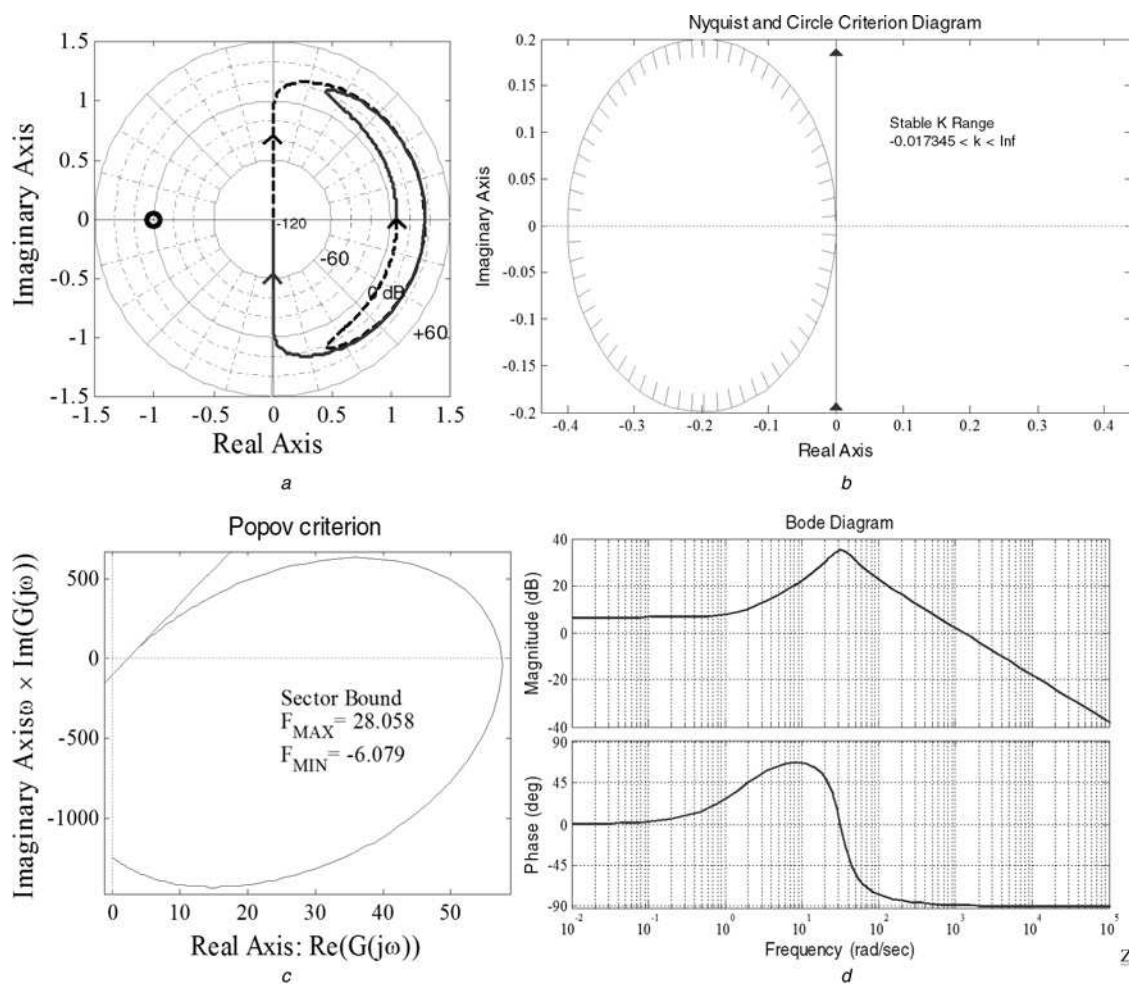


Fig. 9 Stability analysis of the proposed system based on

- a Logarithmic Nyquist method
- b Nyquist and circle test
- c Popov criterion
- d Bode plot

controllers decrease with the decrease of wind power generation and the HS needs larger gain values to meet the reactive power mismatch. It is also noted that the peak value of ΔV varies in accordance with the size of the Wind and PV system. It is worth noticing that the reactive power need was first met by the SG and in subsequent time it was met by the FACTS devices. Maximum deviations of different parameters with 2% step increase of load is shown in Table 2. The responses of all the system parameters are clearly depicted in the figures showing their settling time and peak overshoots, and thereby proving clearly the superiority of UPFC than other devices.

3.2 System stability analysis of the system

For stability analysis a polar diagram is represented in Fig. 9a, where the amplitude of the system transfer function is plotted in logarithm scale. Here the stability analysis is performed based on the encirclements of the poles on the imaginary axis, gain and phase margins. Usually spirals shown in the RHP do not overlap with the polar plot. Based on the no of encirclements about the poles the stability of the HS is determined. Then, the stability study based on Nyquist criterion is represented in Fig. 9b. Based on this criterion, the HS become stable for the range of k for which $-1/k$ do not lie in the right half of s-plane. The range of k determined from the criterion for which the system becomes stable is $-0.017345 < k < \text{Inf}$. Further to support the stability study popov and bode diagrams are plotted in Figs. 9c and d. According to the Popov criterion, the minimum ($F_{\text{Min}} = -6.079$) and maximum ($F_{\text{Max}} = 28.058$) of an

auxiliary function is determined to know the stability of the system. Again magnitude and frequency bode plot show the gain margin and phase margin which defines the stability of HS.

4 Conclusion

Reactive power compensation of isolated wind–diesel-PV HS has been simulated with the incorporation of SVC, STSTCOM and UPFC. It is observed from the simulation results that transient voltage stability in case of UPFC is better as compared with that of SVC and STATCOM. Further, the transient stability study in HS is also analysed with UPFC based on fuzzy-PI and fuzzy-SMC. It is concluded from the simulation that the performance of UPFC with fuzzy-sliding mode is improved in comparison with the conventional PI and fuzzy-PI controller. In addition, system stability study based on polar diagram, Nyquist, Popov criterion and bode plot is presented which reflects better stability of the proposed controller. Again quantitative analysis based on settling time and peak overshoot is represented. Both qualitative and quantitative analysis proved the robustness of the proposed Fuzzy-Sliding mode based UPFC controller under varying operating condition.

5 Acknowledgments

The author, Asit Mohanty would like to thank Dr. Meera Viswavandya, Associate Professor CET Bhubaneswar for her

constant support and guidance for carrying out the research work. He is also indebted to Prof. P.K. Patra Principal CET Bhubaneswar for creating an atmosphere conducive for advance research work. The authors are also thankful to Dr. Soumya R. Mohanty, Assistant Professor, MNNIT Allahabad for his meticulous guidance, constructive and valuable suggestions.

6 References

- 1 Jeon, J., Kim, S., Cho, C., *et al.*: 'Development of a grid-connected Wind/PV/BESS hybrid distributed generation system'. Presented at the 19th Int. Conf. Elect. Distrib. (CIRED), Vienna, Austria, 21–24 May 2007
- 2 Onara, O.C., Uzunoglu, M., Alama, M.S.: 'Modeling, control and simulation of an autonomous wind turbine/photovoltaic/fuel cell/ultracapacitor hybrid power system', *J. Power Sources*, 2008, **185**, (2), pp. 1273–1283
- 3 Bansal, R.C., Bhatti, T.S., Kumar, V.: 'Reactive power control of autonomous wind diesel hybrid power system using ANN'. Proc. IEEE Power Engineering Conf., 2007
- 4 Bansal, R.C.: 'Three phase self-Excited Induction Generators, an over view', *IEEE Trans. Energy Convers.*, 2005, **20**, (2), pp. 292–299
- 5 Bansal, R.C.: 'Automatic reactive power control of autonomous hybrid power system'. PhD Thesis, Centre for Energy Studies, IIT Delhi, December 2002
- 6 Lee, D.-J., Wang, L.: 'Small signal stability analysis of an autonomous hybrid renewable energy power generation/energy storage system part I: Time domain simulations', *IEEE Trans. Energy Convers.*, 2008, **23**, (1), pp. 311–320
- 7 Douglas, J.F.H.: 'Characteristics of induction motors with permanent magnet excitation', *TransAIEE(PAS)*, 1959, **178**, pp. 221–225
- 8 Kaldellis, J.K., Zafirakis, D., Kavadias, K.: 'Autonomous energy system for remote island based on renewable energy sources'. Proc. EWEC 99, Nice, 1999
- 9 Murthy, S.S., Malik, O.P., Tondon, A.K.: 'Analysis of Self Excited Induction Generator'. IEE Proc, November 1982, vol. 129
- 10 Hingorani, N.G., Gyugyi, L.: 'Understanding FACTS, concepts and technology of flexible AC transmission system' (IEEE Power Engineering Society, New York, 2000)
- 11 Padiyar, K.R.: 'FACTS controlling in power transmission system and distribution' (NewAge International Publishers, 2008)
- 12 Hammad, A.E., El Sadek, M.: 'Application of thyristor controlled var compensator for damping sub synchronous oscillation in power system', *IEEE Trans. Power Appl. Syst.*, 1984, **103**, (1), pp. 198–212
- 13 Saha, T.K., Kasta, D.: 'Design optimisation & dynamic performance analysis of electrical power generation system', *IEEE Trans. Energy Convers. Device*, 2010, **25**, (4), pp. 1209–1217
- 14 Rao, P., Crow, M.L.: 'STACOM Control for power application'. Proc. North American Power Symp. (NAPS), 1997, pp. 172–178
- 15 Koudri, B., Tahir, Y.: 'Power flow and transient stability Modelling of a 12 pulse STATCOM', *J. Cybermatics Inf.*, 2008, **7**, pp. 9–25
- 16 Fukami, T., Nakagawa, K., Kanamaru, Y., *et al.*: 'Performance analysis of permanent magnet Induction generator under unbalanced grid voltages', *Translated from Denki GakkiRonbunsi*, 2006, **126**, (2), pp. 1126–1133
- 17 Padiyar, K.R., Verma, R.K.: 'Damping torque analysis of static VAR system controller', *IEEE Trans. Power Syst.*, 1991, **6**, (2), pp. 458–465
- 18 Uzunovic, E., Canizares, C.A., Reeve, J.: 'EMTP studies of UPFC power oscillation damping'. Proc. NAPS, San Luis Obispo, California, October 1999, pp. 405–410
- 19 Majumder, R.: 'Modeling, stability analysis and control of microgrid'. Ph.D. dissertation, Queensland Univ. Technol., Brisbane, Australia, 2010
- 20 Tzung-Lin, L., Shang-Hung, H., Yu-Hung, C.: 'Design of D-STATCOM for voltage regulation in microgrids'. Proc. IEEEECCE, 12–16 September 2010, pp. 3456–3463
- 21 Balaguer, I.J., Qin Lei, L., Shuitao, Y., *et al.*: 'Control for grid-connected and intentional islanding operations of distributed power generation', *IEEE Trans. Ind. Electron.*, 2011, **58**, (1), pp. 147–157
- 22 Panda, S., Padhy, N.P.: 'Power system with PSS and FACTS controller: modeling, simulation and simultaneous tuning employing genetic algorithm', *Int. J. Electr. Electron. Eng. I*, 2007, **1**, (1), pp. 9–18
- 23 Tambey, N., Kothari, M.L.: 'Damping of power system oscillations with unified power flow controller (UPFC)', *IEE Proc.-Gener. Transm. Distrib.*, 2003, **150**, (2), pp. 129–140
- 24 Talaq, J., Al-Basri, F.: 'Adaptive fuzzy gain scheduling for load frequency control', *IEEE Trans. Power Syst.*, 1999, **14**, (1), pp. 145–150
- 25 Chang, C.S., Fu, W.: 'Area load frequency control using fuzzy gain scheduling of PI controllers', *Electr. Power Syst. Res.*, 1997, **42**, (2), pp. 145–152
- 26 Fosha, C.E., Elgerd, O.I.: 'The megawatt-frequency control problem: a new approach via optimal control theory', *IEEE Trans. Power Appar. Syst.*, 1970, **PAS-89**, (4), pp. 563–577
- 27 Pan, C.T., Liaw, C.M.: 'An adaptive controller for power system load-frequency control', *IEEE Trans. Power Syst.*, 1989, **4**, (1), pp. 122–128
- 28 Sivaramakrishnan, A.Y., Hariharan, M.V., Srisailam, M.C.: 'Design of variable-structure load-frequency controller using pole assignment technique', *Int. J. Control*, 1984, **40**, (3), pp. 487–498

- 29 Al-Hamouz, Z.M., Abdel-Magid, Y.L.: 'Variable structure load frequency controllers for multiarea power systems', *Int. J. Electr. Power Energy Syst.*, 1993, **15**, (5), pp. 293–300
- 30 Saadat, H.: 'Power system analysis' (Mc-Graw Hill, 1999)
- 31 Dhanalakshmi, R., Palaniswami, S.: 'ANFIS based Neuro-Fuzzy Controller in LFC of Wind-Micro Hydro-Diesel Hybrid Power System', *Int. J. Comput. Appl.*, 2012, **42**, (6), pp. 28–35
- 32 Mohanty, A., Viswawandya, M., Ray, P.K., *et al.*: 'Stability analysis and reactive power compensation issue in a microgrid with a DFIG based WECS', *Int. J. Electr. Power Energy Syst., Elsevier Sci*, 2014, **62**, pp. 753–762

7 Appendix

See Tables 1–4.

Table 1 Optimum gain setting of FACTS devices for proposed HS

Wind-diesel-PV hybrid system	Constant slip		Variable slip	
	K_P	K_I	K_P	K_I
with SVC	500	6000	390	5000
with STATCOM	35	6100	31	4900
with UPFC	31	5500	29	4760

Table 2 Maximum deviations of different parameters with 2% step increase of load

S. no	Controllers	ΔV	ΔQ_{SG}	ΔQ_{PV}	ΔQ_{COM}	ΔQ_G
1	SVC	-0.0018	0.01381	0.012	0.026	-0.003
		-0.0019	0.01451	0.011	-0.025	-0.002
2	STATCOM	-0.0009	0.0067	0.008	0.021	-0.002
		-0.0008	0.0071	0.009	-0.023	-0.001
3	UPFC	-0.0006	0.0054	0.006	0.018	-0.002
		-0.0005	0.0060	0.007	-0.019	-0.001

Table 3 Parameters of the system

Parameters of wind-diesel-PV system			
System Parameter	Wind-diesel-PV system		
wind capacity (In KW)	150 KW		
diesel capacity (In KW)	150 KW		
PV capacity (In KW)	150 KW		
load capacity (In KW)	250 KW		
base power (In KVA)	250		
synchronous generator			
P_{SG}	0.4	V (PU)	1
Q_{SG}	0.2	X_d (pu)	1
E_d	1.113	$T_{do,s}$	5
E_d	0.96		
induction generator		P_{IN} (PU) in KW	0.75
P_{IG} (PU) in KW	0.6	$r1 = r2$ (PU)	0.19
Q_{IG} (PU) in KVAR	0.189	$X_1 = X_2$ (PU)	0.56
load		Q_L (PU) in KVAR	0.75
P_L (PU) in KW	1.0	α in radian	2.44

Table 4 Parameters of the system

Parameters of FACTS controllers					
SVC		STATCOM		UPFC	
T_α (S)	0.005	T_α (S)	0.2–0.3	T_α (S)	0.05
T_d (s)	0.0016	T_d (s)	1.67	T_{do}	5.044
				X_d	0.3